



OPEN

## Highly diastereoselective cascade [5 + 1] double Michael reaction, a route for the synthesis of spiro(thio)oxindoles

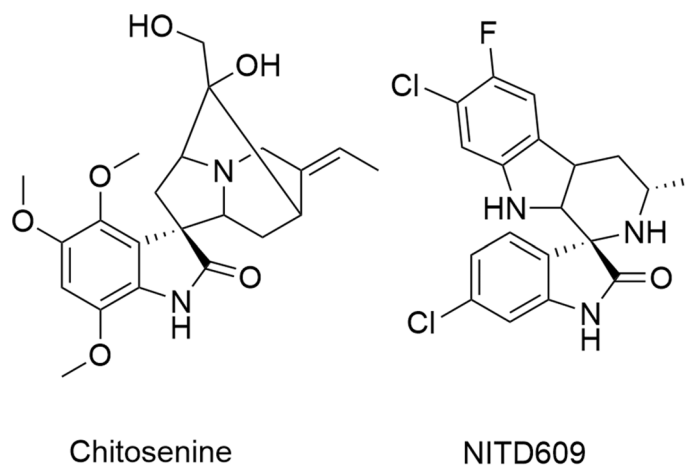
Firouz Matloubi Moghaddam<sup>1✉</sup>, Vahid Saberi<sup>1</sup> & Ashkan Karimi<sup>1,2</sup>

The first diastereoselective synthesis of spirothiooxindoles is reported via the Michael reaction between thiooxindoles and dibenzalacetones. The reaction was conducted without any catalyst or additive under green conditions, i.e., ethanol as the solvent and at room temperature. In addition, the described robust method benefits from scalability, simple work-up, and column chromatography-free purification. This work demonstrates the art of governing regio- and stereoselectivity, which has been discussed in the light of Density Functional Theory calculations. Our method represents the first synthesis of spiro[cyclohexanone-thiooxindoles] with the relative configuration of the aryl moieties at the cyclohexanone ring as *cis*. The obtained *cis*-spirothiooxindoles, can be used to afford *cis*-spirooxindoles, which their synthesis had not been explored before. According to our molecular docking studies, *cis*-spirooxindoles demonstrate higher binding affinities than corresponding *trans*-spirooxindoles for the OPRT domain of the *Leishmania donovani* uridine 5'-monophosphate synthase (LdUMPS). Thus, the reported method may eventually be utilized to develop new hit compounds for leishmaniasis treatment.

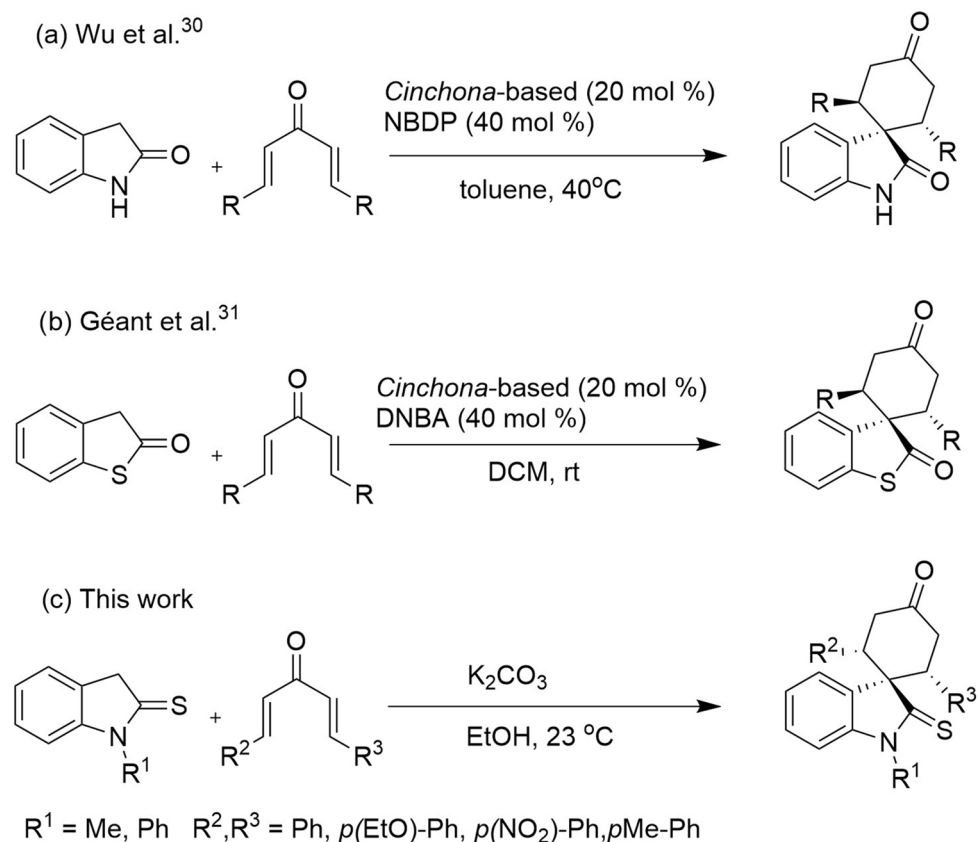
Oxindole scaffolds are a vital pharmacophore<sup>1</sup>, encountered in natural products<sup>2,3</sup> and pharmaceutical compounds. Inspired by the presence of spirooxindole scaffolds in several natural products such as gelsemine, chitosenine, spirotryprostatin B, and NITD609<sup>4–11</sup> (Fig. 1), it is speculated that introducing a tetrahedral spiro carbon can further improve bioactivity by providing structural rigidity<sup>12</sup>. Consequently, there have been numerous efforts made towards synthesizing heterocycles containing spirooxindole as the core structure<sup>13–18</sup>. Among different methodologies developed for synthesizing spirocyclic compounds<sup>19,20</sup>, the Michael addition is one of the most robust<sup>21–24</sup>. Recently, the organocatalytic cascade Michael addition has emerged as an efficient strategy for synthesizing spirooxindoles in one-pot<sup>25–29</sup>. For example, Wu et al. demonstrated a cascade [5 + 1] double Michael addition between dibenzalacetones and oxindoles<sup>30</sup> to afford spiro[cyclohexanone-oxindole] derivatives (Fig. 2a). Later, Géant et al. applied a tandem [5 + 1] double Michael addition, obtaining spiro[cyclohexanone-benzothioindole] derivatives with high optical purity (Fig. 2b)<sup>31</sup>.

However, despite all previous efforts to synthesize spiro[cycloalkane-oxindole] compounds with the relative configuration of the aryl moieties at the cycloalkane ring as *trans* (*trans*-spirooxindoles), the synthesis of *cis*-spirooxindoles has remained unexplored. Since previous biological studies have only focused on *trans*-spirooxindoles, the *cis* isomer could be a demanding target for synthesis as it may further expand the biological activities of oxindoles. For example, Scala et al. discovered *trans*-spiro[cyclohexanone-oxindole] derivatives are efficient inhibitors that kill *Leishmania infantum* promastigotes and amastigotes without significant cytotoxic effects<sup>32</sup>. More evidence for the high activity of spirooxindoles against leishmaniasis were confirmed by Saha et al.<sup>33</sup>. The leishmaniasis are a group of diseases caused by protozoan parasites from more than 20 *Leishmania* species<sup>34</sup>. A better understanding of leishmaniasis was provided when French et al. demonstrated that *L. donovani* uridine 5'-monophosphate synthase (LdUMPS) is an essential enzyme for promastigotes viability and presented the crystal structure of the LdUMPS in complex with its product, UMP<sup>35</sup>. Their structural analysis revealed a tetrameric structure for LdUMPD with two dimeric OMPDC and two dimeric OPRT functional domains. As a result of this unusual structure, the oligomerization of LdUMPS is controlled by ligand binding at the OPRT active site.

<sup>1</sup>Laboratory of Organic Synthesis and Natural Products, Department of Chemistry, Sharif University of Technology, Tehran 111559516, Iran. <sup>2</sup>Department of Chemistry, McGill University, Montreal H3A-0B8, Canada. ✉email: matloubi@sharif.edu

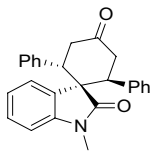
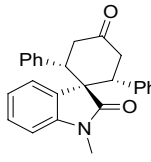
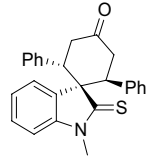
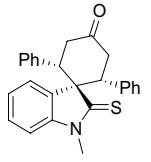


**Figure 1.** Biologically active natural products with a spirooxindole scaffold.



**Figure 2.** Comparison of different cascade [5 + 1] double Michael additions of dibenzalacetones on (thio)oxindoles.

Regarding the structure–activity relationship, we hypothesized a *cis*-spiro[cyclohexanone-(thio)oxindole] might have a higher affinity for the OPRT domain of LdUMPS than the *trans* isomer. To test this hypothesis, some docking studies were initially done, and then a method to synthesize *cis*-spirothiooxindoles was introduced (Fig. 2c). In the next step and in continuation of our previous works on oxindole chemistry<sup>36,37</sup>, thiooxindole was employed to react with dibenzalacetones. The highly diastereoselective [5 + 1] double Michael addition resulted in *cis*-spiro[cyclohexanone-thiooxindoles], which could then be converted to *cis*-spiro[cyclohexanone-oxindoles]. Finally, density functional theory (DFT) was used to explain the reaction regioselectivity and stereoselectivity.

			
<b>1</b>	<b>2</b>	<b>3</b>	<b>4</b>
-7.30 kcal mol <sup>-1</sup>	-7.90 kcal mol <sup>-1</sup>	-6.80 kcal mol <sup>-1</sup>	-7.50 kcal mol <sup>-1</sup>

**Table 1.** Calculated binding energies (kcal mol<sup>-1</sup>) of *trans/cis*-spirocyclic (thio)oxindoles with OPRT domain of LdUMPS.

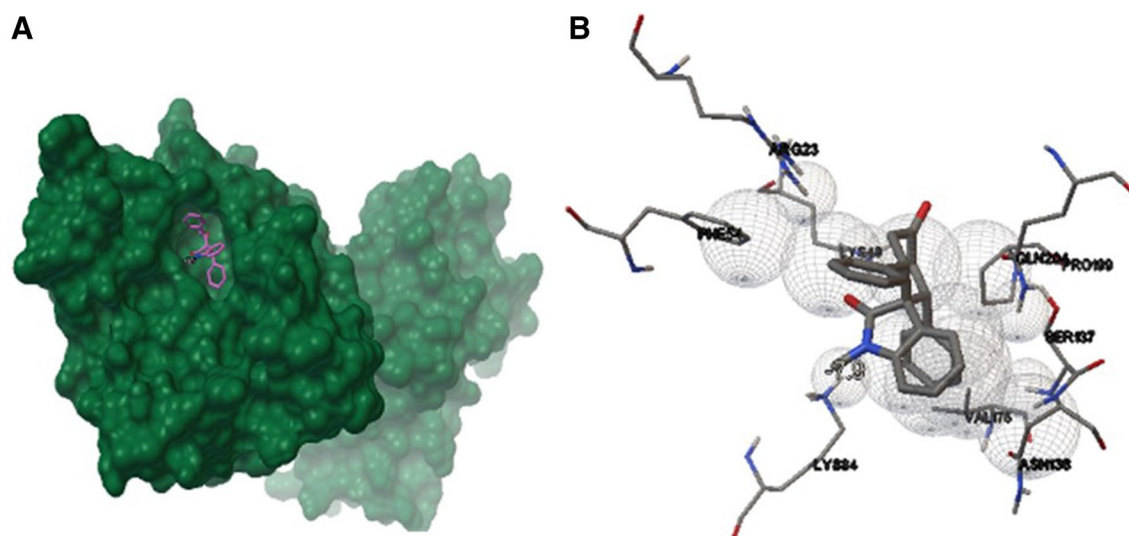


**Figure 3.** Interaction between *cis*-spirooxindole 2 with (A) OPRT domain of the LdUMPS (PDB ID: 2WNS) and (B) residual amino acids of the active site, which include Arg23, Phe54, Lys84, Asn138, Val175, Ser137, Pro199, Gln204, and Lys49. The figure was drawn using UCSF chimera 1.8 (<https://www.cgl.ucsf.edu/chimera>) and AutoDockTools version 1.5.6 (<http://autodock.scripps.edu>)<sup>38,39</sup>.

## Result and discussion

To gain insight into the molecular determinants that can modulate the antagonistic activities of oxindoles and thiooxindoles, we performed molecular docking studies on *cis* and *trans* isomers. The results generated based on the crystal structure of the LdUMPS receptor, revealed that *cis*-spiro[cyclohexanone-oxindole] 2 (*cis*-spirooxindole) has the highest binding affinity for the LdUMPS active site (Table 1). It binds to the OPRT domain of the LdUMPS receptor through interactions with Arg23, Phe54, Lys84, Asn138, Val175, Ser137, Pro199, Gln204, and Lys49 (Figs. 3 and S1). The higher binding energy of *cis*-spirooxindole 2 than the *trans* isomer 1 relies on steric hindrance between *trans*-spirooxindole and the active site. Electronic factors seem responsible for the higher activity of *cis*-oxindole 2 in comparison with *cis*-thiooxindole 4.

Motivated by the initial docking results, which confirmed the importance of designing a robust synthetic method to provide *cis*-oxindole 2, we, therefore, commenced the synthesis design. Since all previously applied Michael reactions on oxindole have thus far resulted in the *trans* isomer 1 formation, it was hypothesized that replacing the carbonyl group of the oxindole with a thiocarbonyl group may introduce an intramolecular repulsion between the large lone-pair electrons of sulfur and aryl  $\pi$  electrons. This could favor the formation of *cis*-thiooxindole 4, which after one extra step could be converted to *cis*-oxindole 2. Theoretical calculations confirmed this hypothesis. The DFT computations (Fig. 4) demonstrated that the *cis* isomer 4 is more thermodynamically stable than the *trans* isomer 3 (Table S1), due to the electronic repulsion. These results also explain why previous works on oxindoles, where the *trans* isomer 1 is more stable than the *cis* isomer 2, could only achieve the *trans* isomer.

In the following step, thiooxindole derivatives were generated from the reaction of oxindole with P<sub>2</sub>S<sub>5</sub> and sodium bicarbonate in dry THF. dibenzalacetone derivatives were prepared through the condensation reaction of acetone and aryl aldehydes in the presence of a suitable base with ethanol as the solvent. The [5 + 1] double Michael addition reaction was conducted with an equimolar mixture of freshly prepared thiooxindole 6 with dibenzalacetone to provide the single diastereomer 7 in high yield. The product is not soluble in the reaction

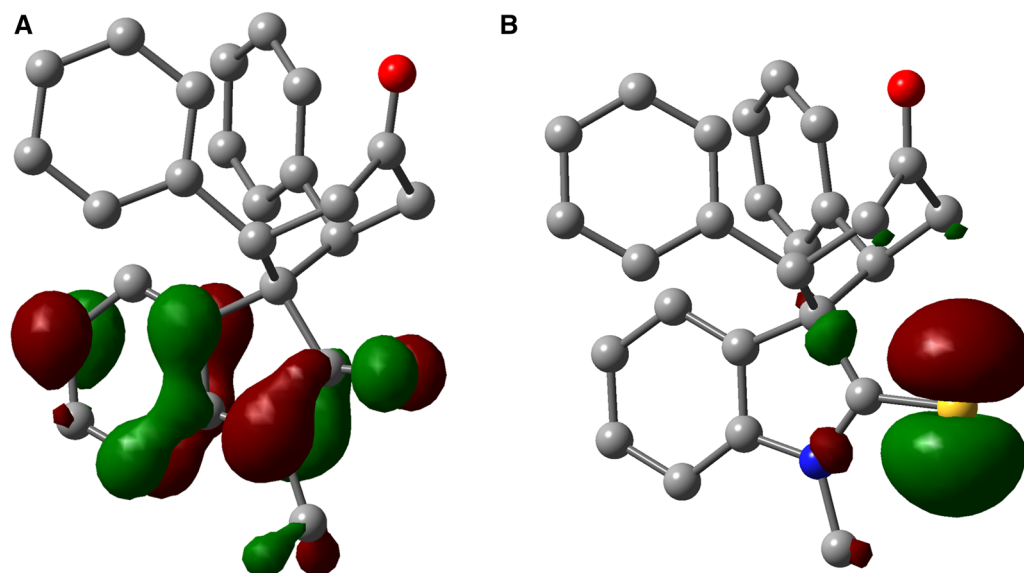


**Figure 4.** HOMO electronic cloud of (A) *cis*-spirooxindole **2** and (B) *cis*-spirothiooxindole **4**. The diffusive electronic cloud around the sulfur atom in thiooxindole makes the *cis* isomer to be more stable than the *trans* isomer. DFT calculations were performed using B3LYP/6-31+G(d) in the gas phase. The figure was drawn using GaussView version 6.1.1 (<https://gaussian.com/gaussview6>)<sup>40</sup>.

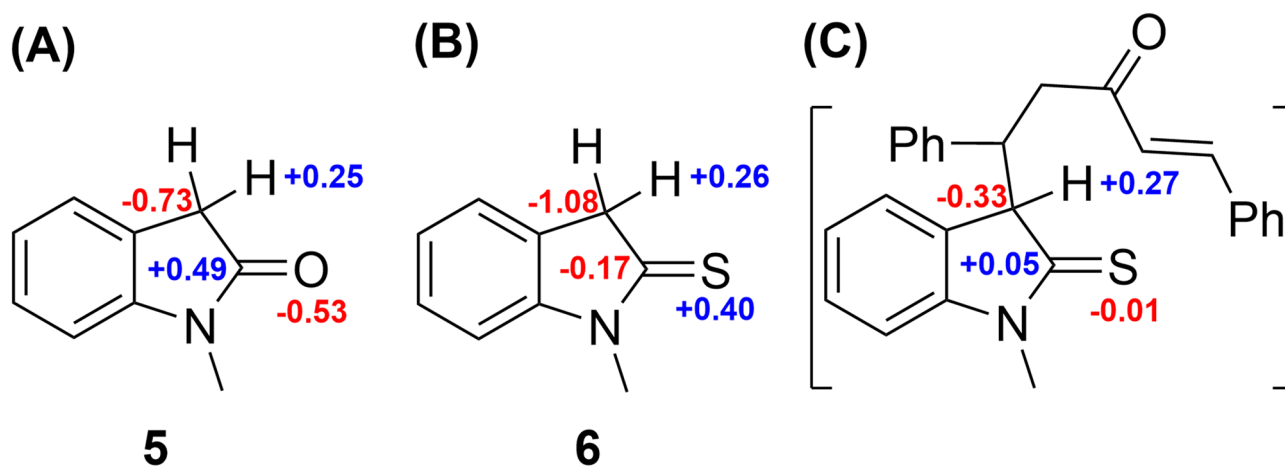
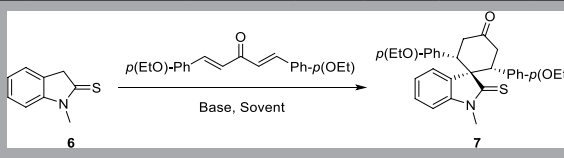


**Figure 5.** Mulliken charge distribution on (A) N-methyl oxindole **5**, (B) N-methyl thiooxindole **6** and (C) the intermediate after the first Michael addition on N-methyl thiooxindole **6**. Calculations were performed using B3LYP/6-31G(d) in the gas phase.

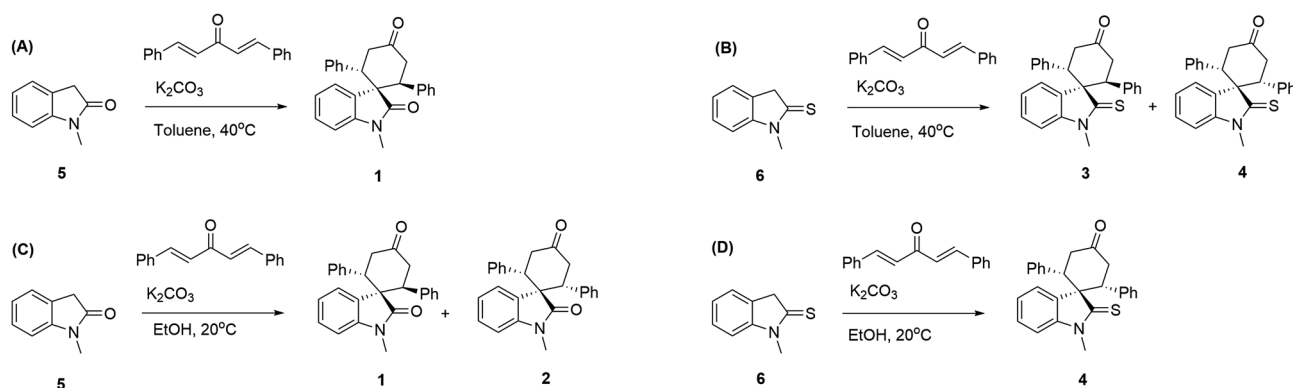
solvent—ethanol—thus, we could isolate the pure product by filtration followed by washing it with ethanol and diethyl ether. The regio- and diastereoselectivity of this reaction were established by the aim of the one- and two-dimensional NMR. In <sup>1</sup>H-NMR, compound **7** displayed two doublets at  $\delta$  6.55 and 6.65 ppm, equivalent to four protons for each signal. This confirmed the *p*-ethoxyphenyl groups of the thiooxindole moiety exist at the *cis* position with respect to each other. In the <sup>1</sup>H and <sup>13</sup>C-NMR spectra, no signal was observed related to other diastereomers. Further analysis by COSY, NOESY, and single-crystal X-ray diffraction, revealed that the aryl groups stand toward the phenyl part of thiooxindole.

Initially, the obtained regioselectivity of this reaction was a surprise as one could expect to observe the Michael addition on alpha carbon and sulfur, which results in the formation of an eight-member ring. To explain the observed regioselectivity, we used DFT calculations. Considering the charge distribution (Fig. 5), we noticed the alpha carbon of thiooxindole is more electron-rich than sulfur—even after the first Michael addition (Fig. 5C)—and thus can act as a better nucleophile. Furthermore, the alpha carbon of thiooxindole **6** is more electron-rich than the alpha carbon of oxindole **5**. Accordingly, thiooxindole **6** is a better Michael donor than oxindole **5**. This trend is in agreement with the strong resonance between the nitrogen atom and the carbonyl group in oxindole, whereas in thiooxindole there is a stronger resonance between the alpha carbon and the



Entry	Base	Solvent	Temperature (°C)	Yield <sup>b</sup> (%)	Entry	Base	Solvent	Temperature (°C)	Yield <sup>b</sup> (%)
1	K <sub>2</sub> CO <sub>3</sub> <sup>c</sup>	EtOH	23	21	7	K <sub>2</sub> CO <sub>3</sub>	Toluene <sup>c</sup>	23	31f.
2	K <sub>2</sub> CO <sub>3</sub>	EtOH	23	81	8	K <sub>2</sub> CO <sub>3</sub>	THF	23	Trace
3	K <sub>2</sub> CO <sub>3</sub> <sup>d</sup>	EtOH	23	56	9	K <sub>2</sub> CO <sub>3</sub>	H <sub>2</sub> O	23	Trace
4	–	EtOH	23	–	10	K <sub>2</sub> CO <sub>3</sub>	MeOH	23	Trace
5	DABCO	EtOH	23	20	11	K <sub>2</sub> CO <sub>3</sub>	DCM	23	Trace
6	NaOH	EtOH	23	Trace	12	K <sub>2</sub> CO <sub>3</sub>	EtOH	Reflux	36

**Table 2.** Optimization of the double Michael addition reaction conditions. <sup>a</sup>0.5 mmol thioxindole (1.0 eq), 0.5 mmol dibenzalacetone (1.0 eq), 0.5 mmol base (1.0 eq), 20 mL solvent. <sup>b</sup>Isolated yield. <sup>c</sup>0.025 mmol base (0.5 eq) was used. <sup>d</sup>0.5 mmol L-Proline (1.0 eq) was used as an organocatalyst. <sup>e</sup>Mixture of *cis* and *trans* products was obtained. <sup>f</sup>Isolated yield of the *cis* product.

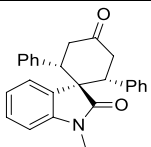
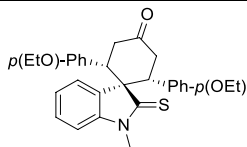
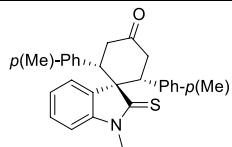
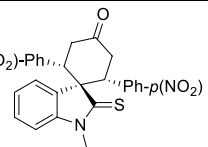
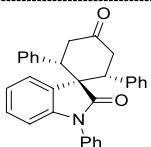
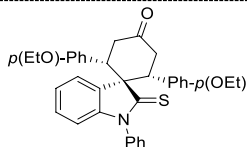
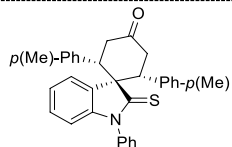
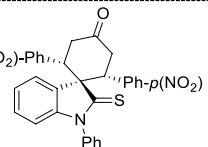


**Figure 6.** Double Michael addition reaction of N-methyloxindole and N-methylthioxindole on dibenzalacetone in different solvents.

thiocarbonyl group. Therefore, the charge distribution explains the formation of the spirocyclic scaffold over the eight-membered ring compounds.

Based on these results, we conducted various experiments to obtain the optimal reaction conditions using the reaction mentioned above as the model (Table 2). The results showed that K<sub>2</sub>CO<sub>3</sub> accelerates the deprotonation step and thus makes the reaction proceed faster. The efficiency of this process could be further improved by increasing the amount of base up to 100 mol%. Moreover, exploring the effect of temperature showed that if the reaction was carried out in ethanol at a higher temperature (reflux condition), the yield of compound 7 would decrease. This temperature effect was predictable based on the negative entropy change for this reaction. We also studied the effect of L-Proline in the reaction, which resulted in a lower yield. Initially, it was expected that L-Proline would accelerate the reaction by forming dibenzaliminium intermediate. However, DFT calculations revealed that the beta carbon of dibenzaliminium is more electron-rich than the beta carbon of dibenzalacetone (Fig. S2), and thus the latter is a better Michael acceptor.

In the next step, the solvent effect on the reaction was surveyed. As an aprotic and apolar solvent, toluene has been previously used to convert oxindole 5 to *trans*-spirooxindole 1 (Fig. 6A). However, the same reaction condition on thioxindole 6, resulted in a mixture of *cis*- and *trans*-spirocyclic products 3 and 4 (Fig. 6B). We, therefore, introduced a method using ethanol as a polar and protic solvent that produces *cis*-spirothioxindole 4 as a single diastereomer (Fig. 6D). Significantly, treating oxindole 5 under our reaction condition resulted in a mixture of *cis*- and *trans*-spirooxindole 1 and 2 (Fig. 6C). Therefore, we concluded both solvent and substrate electronic structure are involved in the determination of reaction diastereoselectivity. To better understand these effects, conductor-like polarizable continuum model (CPCM)<sup>41</sup> was used in our DFT calculations. The theoretical results (Fig. S3) revealed *trans* configuration is more favorable in toluene, whereas the *cis* configuration can form easier in ethanol. This selectivity comes from the fact that the energy level of molecular orbitals and thus the repulsion between the chalcogen lone-pair electrons and  $\pi$  electrons of aryl groups depends on the solvent dielectric constant. Thus, the double Michael addition on oxindole (or thioxindole) in ethanol (or toluene) resulted in selective formation of compound 1 (or 4). However, when the reaction was performed on

 <b>4</b> Yield: 72% -7.90 kcal mol <sup>-1</sup>	 <b>7</b> Yield: 81% -8.11 kcal mol <sup>-1</sup>	 <b>8</b> Yield: 69% -7.85 kcal mol <sup>-1</sup>	 <b>9</b> Yield: 21% -5.58 kcal mol <sup>-1</sup>
 <b>10</b> Yield: 62% -7.05 kcal mol <sup>-1</sup>	 <b>11</b> Yield: 79% -7.26 kcal mol <sup>-1</sup>	 <b>12</b> Yield: 20% -7.15 kcal mol <sup>-1</sup>	 <b>13</b> Yield: 15% -4.59 kcal mol <sup>-1</sup>

**Table 3.** Double Michael addition of thiooxindole on dibenzalacetone, reaction yield, and binding energies (kcal mol<sup>-1</sup>) with OPRT domain of LdUMPS.

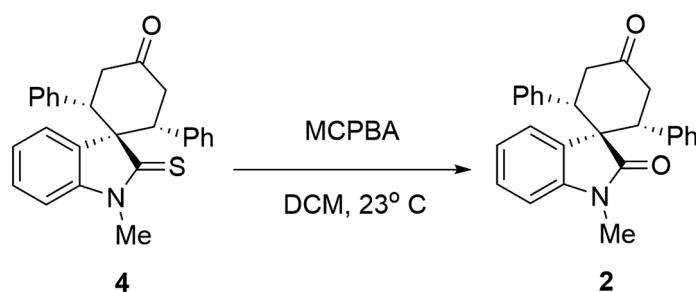


**Figure 7.** Conversion of *cis*-spirothiooxindole into *cis*-spirooxindole.

oxindole in toluene or on thiooxindole in ethanol, the solvent and electronic effects conflicted with each other, and a mixture of *cis* and *trans* isomers was obtained.

To further illustrate the scope of this reaction for the synthesis of complex heterocyclic spirothiooxindoles, N-methylthiooxindole and N-phenylthiooxindole with dibenzalacetone bearing electron-donating or -withdrawing groups were used. The obtained results are summarized in Table 3. In all cases, the reaction furnished a single diastereomer of spirothiooxindoles in moderate to good yields. Furthermore, we successfully scaled up the reaction and isolated > 35 g of compound 7 with 66% yield.

The potential of synthesized compounds as inhibitors of LdUMPS was then recognized by molecular docking (Table 3). Our study showed that compound 7 fits better into the active site of the receptor. N-phenyl derivatives sterically intercut this fitting, and, as a result, they have a lower binding affinity. Finally, we demonstrated that it is possible to convert synthesized spirocyclic thiooxindoles into oxindoles (Fig. 7). Thus, our method opens a new window in the formation of biologically important *cis*-spirooxindoles and *cis*-spirothiooxindoles.

## Conclusion

In summary, we have introduced a robust synthetic strategy for diastereomerically-pure spiro[cyclohexanone-thiooxindole] compounds via double Michael addition of thiooxindoles on dibenzalacetone. The reaction furnished corresponding spiro products in only one diastereomer. The regioselectivity and stereoselectivity of the reaction were discussed in the light of the computational results. Molecular docking studies were performed on the reaction products, which demonstrated high binding affinities for the OPRT domain of the LdUMPS receptor. Our catalyst-free protocol is scalable, has mild reaction conditions, and does not need column chromatography for purification. These advantages make this method a suitable candidate for synthesizing complex spirocyclic oxindoles and thiooxindoles with potential applications in medicinal chemistry.



## Methods

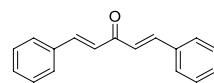
**General information.** All materials used are commercially available and were purchased from Merck and used without any additional purification.  $^1\text{H}$  NMR,  $^{13}\text{C}$  NMR, and 2-D NMR spectra were recorded on a Bruker (Avance DRX-500) spectrometer using  $\text{CDCl}_3$  or  $\text{DMSO-d}_6$  as solvent at room temperature. Chemical shifts ( $\delta$ ) are given in parts per million (ppm) and are reported relative to residual solvent peaks:  $\text{CDCl}_3$  ( $\delta\text{H}$  7.26,  $\delta\text{C}$  77.16 ppm),  $\text{DMSO-d}_6$  ( $\delta\text{H}$  2.50,  $\delta\text{C}$  39.52 ppm). Coupling constants ( $J$ ) are given in Hertz (Hz). FTIR spectra of samples were taken using an ABB Bomem MB-100 FTIR spectrophotometer. HRMS analyses were performed using a TOF mass analyzer on Mat95XP-Trap apparatus. X-ray crystallography was carried out through APEX II CCD BRUKER detector.

**Computational studies.** In all calculations, B3LYP DFT functional theory<sup>42</sup> and 6-31G(d) basis set<sup>43</sup> was used. Calculations were performed in the gas phase or solution by CPCM model and at 298.15 K. Conformer distribution was studied by Spartan04 (<https://www.wavefun.com>)<sup>44</sup> and Gaussian16 revision A.03 (<https://gaussian.com/gaussian16>)<sup>45</sup> was used for other calculations. The first frequency was utilized to assess whether structures were in the true optimized structure. The docking study was performed by using the Autodock 1.5.6. The size of the grid box was set to 20 Å. The enzyme structure was downloaded from the website protein data banks (PDB ID: 2WNS) and ligands optimized at 6-31G(d)-B3LYP level of theory by Gaussian. Auto Dock tools programs were used to visualize the complex in 3D. All single bonds of residue side chains inside the grid box were regarded as rotatable, and the docked ligand was allowed to rotate on all the single bonds and move flexibly within the grid box. The structural optimization was performed for 50,000 generations using a genetic algorithm.

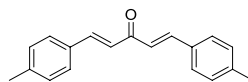
**Single crystal X-ray diffraction.** A single crystal of the compound **11** was mounted on a Kapton loop using a Paratone oil and analyzed by single crystal X-ray diffraction. An APEX II CCD BRUKER detector and a graphite Mo-K $\alpha$  monochromator were used for the data acquisition. All measurements were done at 150 K and a refinement method was used for solving the structure. The structure resolution was accomplished using the SHELXT-2014 program and the refinement was done with the SHELXL-2014/7 program<sup>46,47</sup>. The structure solution and the refinement were achieved with the PLATON software (<http://www.platonsoft.nl/platon>)<sup>48</sup>. Finally, pictures of the compound structure were obtained using the MERCURY 3.08 software (<https://mercury1.softw are.informer.com>)<sup>49</sup>. During the refinement steps, all atoms-except hydrogens-were refined anisotropically. The position of the hydrogens was determined using residual electronic densities which are calculated by a Fourier difference. Finally, in order to obtain a complete refinement, a weighting step followed by multiples loops of refinement was done. The R1 factor and the completeness are indicators of a complete refinement but also a good estimation of the quality of the experimental data.

**General procedure for the synthesis of dibenzalacetones.** Preparation of dibenzalacetone from solid aryl aldehyde: A mixture of  $\text{LiClO}_4$  (5 mmol),  $\text{Et}_3\text{N}$  (5 mmol), acetone (5 mmol), and aryl aldehyde (5 mmol) in 20 mL ethanol as solvent was stirred at room temperature. The reaction completion was monitored by TLC. After the completion of the reaction, the solvent was removed by rotatory evaporation at reduced pressure, and the residue was washed by ethanol to afford the pure product.

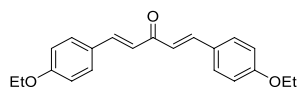
Preparation of dibenzalacetone from liquid aryl aldehyde: A mixture of NaOH (25 mmol), acetone (5 mmol), and aryl aldehyde (5 mmol) in the mixture of  $\text{H}_2\text{O}/\text{EtOH}$  (10:8) was stirred at room temperature for 10 min. The reaction completion was monitored by TLC. After the completion of the reaction, the solvent was removed by rotatory evaporation at reduced pressure, and the residue was washed by ethanol to afford the pure product.



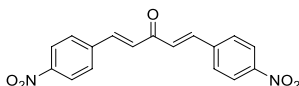
*1,5-Diphenyl-penta-1,4-dien-3-one*: Yellow solid,  $^1\text{H}$  NMR ( $\text{CDCl}_3$ , 500 MHz),  $\delta$  7.02 (2 H, d,  $J = 15.9$  Hz), 7.42 (4 H, dd,  $J = 5.0, 1.8$  Hz), 7.63 (6 H, dd,  $J = 6.4, 3.1$  Hz), 7.75 (2H, d,  $J = 15.9$  Hz). HRMS (ESI):  $m/z$  234.1051 ( $\text{M}^+ \cdot \text{C}_{17}\text{H}_{14}\text{O}^{+}$  requires 234.1039). The spectroscopic data are consistent with those previously reported<sup>50</sup>.



*1,5-Di-p-tolyl-penta-1,4-dien-3-one*: Yellow solid,  $^1\text{H}$  NMR ( $\text{CDCl}_3$ , 500 MHz),  $\delta$  2.35 (6H, s), 7.09 (2H, d,  $J = 15.0$  Hz), 7.29 (4H, d,  $J = 7.5$  Hz, 2H), 7.50 (4H, d,  $J = 7.5$  Hz), 7.92 (2H, d,  $J = 15.2$  Hz). HRMS (ESI):  $m/z$  262.1385 ( $\text{M}^+ \cdot \text{C}_{19}\text{H}_{18}\text{O}^{+}$  requires 262.1352). The spectroscopic data are consistent with those previously reported<sup>50</sup>.



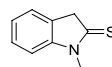
*1,5-Bis(4-ethoxyphenyl)penta-1,4-dien-3-one*: Yellow solid,  $^1\text{H}$  NMR ( $\text{CDCl}_3$ , 500 MHz),  $\delta$  1.44 (6 H, t,  $J=7.0$  Hz), 4.08 (4 H, q,  $J=7.0$  Hz), 6.92 (4 H, d,  $J=8.7$  Hz), 6.95 (2 H, d,  $J=15.9$  Hz), 7.56 (4 H, d,  $J=8.7$  Hz), 7.69 (2H, d,  $J=15.8$  Hz). HRMS (ESI):  $m/z$  322.1574 ( $\text{M}^{++} \text{C}_{21}\text{H}_{22}\text{O}_3^{++}$  requires 322.1563). The spectroscopic data are consistent with those previously reported<sup>50</sup>.



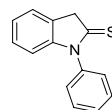
*1,5-Bis(4-nitrophenyl)penta-1,4-dien-3-one*: Brown solid,  $^1\text{H}$  NMR ( $d_6$ -DMSO, 500 MHz),  $\delta$  7.56 (2 H, d,  $J=16.1$  Hz), 7.93 (2 H, d,  $J=16.1$  Hz), 8.08 (4 H, d,  $J=8.5$  Hz), 8.31 (4H, d,  $J=8.5$  Hz). HRMS (ESI):  $m/z$  324.0749 ( $\text{M}^{++} \text{C}_{17}\text{H}_{12}\text{N}_2\text{O}_5^{++}$  requires 324.0746). The spectroscopic data are consistent with those previously reported<sup>50</sup>.

**General procedure for synthesizing thiooxindoles.** An oven-dried flask was charged with oxindole (3.7 mmol), dry THF (25 mL), and  $\text{P}_2\text{S}_5$  (2.3 mmol). The reaction mixture was stirred at room temperature for 10 min. Then,  $\text{NaHCO}_3$  (7.5 mmol) was slowly added and stirred overnight.

After removing the solvent by rotatory evaporation at reduced pressure, the residue was transferred into a 100-mL beaker. By adding 250 mL mixture of ice and water, a pale yellow solid appeared. The light-yellow precipitate was washed with 10% solution of  $\text{NaHCO}_3$  to remove unreacted oxindole and give the pure product.



*1-methylindoline-2-thione (6)*: Yellow solid,  $^1\text{H}$  NMR ( $\text{CDCl}_3$ , 500 MHz),  $\delta$  3.61 (s, 3H), 4.09 (s, 2H), 6.98 (1H, d,  $J=7.8$  Hz), 7.16 (1H, t,  $J=7.4$  Hz), 7.27 (1H, d,  $J=7.8$  Hz), 7.32 (1H, t,  $J=7.8$  Hz). HRMS (ESI):  $m/z$  163.0467 ( $\text{M}^{++} \text{C}_9\text{H}_9\text{NS}^{++}$  requires 163.0450). The spectroscopic data are consistent with those previously reported<sup>51</sup>.



*1-phenylindoline-2-thione*: brown solid,  $^1\text{H}$  NMR ( $\text{CDCl}_3$ , 500 MHz),  $\delta$  4.32 (2 H, s), 6.65 (1 H, d,  $J=7.7$  Hz), 7.20 (1 H, t,  $J=7.32$  Hz), 7.25 (1 H, t,  $J=7.5$  Hz), 7.38 (1 H, d,  $J=7.15$  Hz), 7.43 (2 H, d,  $J=7.5$  Hz), 7.55 (1 H, t,  $J=7.4$  Hz), 7.63 (2 H, t,  $J=7.6$  Hz). HRMS (ESI):  $m/z$  225.0622 ( $\text{M}^{++} \text{C}_{14}\text{H}_{11}\text{NS}^{++}$  requires 225.0607). The spectroscopic data are consistent with those previously reported<sup>52</sup>.

**General procedure for double Michael addition reaction.** A mixture of thiooxindole (0.5 mmol), dibenzalacetone (0.5 mmol), and  $\text{K}_2\text{CO}_3$  (0.5 mmol) in 10 mL of ethanol was stirred at room temperature for about 24 h. Reaction completion was monitored by TLC using mobile phase (ethyl acetate/hexane; 1:6). Since the product is insoluble in ethanol and diethyl ether, the purification was done by washing the crude reaction mixture with these solvents.

*(1s,2R,6S)-1'-methyl-2,6-diphenyl-2'-thioxospiro[cyclohexane-1,3'-indolin]-4-one (4)*: White solid,  $^1\text{H}$  NMR ( $\text{CDCl}_3$ , 500 MHz),  $\delta$  2.82 (2H, dd,  $J=15.7, 4.0$  Hz), 3.00 (3 H, s), 3.46 (2 H, t,  $J=15.1$  Hz), 4.14 (2H, dd,  $J=14.6, 4.2$  Hz), 6.63 (1H, d,  $J=6.9$  Hz), 6.82 (4 H, d,  $J=7.5$  Hz), 6.95 (4 H, d,  $J=7.7$  Hz), 7.32–7.38 (2H, m), 8.02–8.07 (1H, m).  $^{13}\text{C}$  NMR ( $\text{CDCl}_3$ , 125.8 MHz):  $\delta$  34.6, 43.7, 49.8, 67.6, 108.5, 125.5, 127.3, 127.5, 128.13, 128.5, 128.8, 129.5, 139.5, 146.9, 207.7, 208.5. HRMS (EI):  $m/z$  397.1480 ( $\text{M}^{++} \text{C}_{26}\text{H}_{23}\text{NOS}^{++}$  requires 397.1495).

*(1s,2R,6S)-2,6-bis(4-ethoxyphenyl)-1'-methyl-2'-thioxospiro[cyclohexane-1,3'-indolin]-4-one (7)*: White solid,  $^1\text{H}$  NMR ( $\text{CDCl}_3$ , 500 MHz),  $\delta$  1.30 (6 H, t,  $J=7.0$  Hz), 2.75 (2H, dd,  $J=15.6, 3.9$  Hz), 3.00 (3 H, s), 3.39 (2 H, t,  $J=15.1$  Hz), 3.85 (4 H, q,  $J=7.0$  Hz), 4.06 (2H, dd,  $J=14.3, 2.7$  Hz), 6.45 (4 H, d,  $J=8.7$  Hz), 6.64 (1H, d,  $J=6.9$  Hz), 6.71 (4 H, d,  $J=8.7$  Hz), 7.32 (2H, quin,  $J=7.6$  Hz), 7.99 (1H, d,  $J=7.3$  Hz).  $^{13}\text{C}$  NMR ( $\text{CDCl}_3$ , 125.8 MHz):  $\delta$  14.7, 31.1, 45.0, 51.2, 63.1, 68.1, 110.0, 113.3, 123.2, 125.3, 128.8, 129.5, 129.7, 132.6, 146.2, 157.8, 204.7, 208.2. HRMS (EI):  $m/z$  485.2015 ( $\text{M}^{++} \text{C}_{30}\text{H}_{31}\text{NO}_3\text{S}^{++}$  requires 485.2025).

*(1s,2R,6S)-1'-methyl-2'-thioxo-2,6-di-p-tolylspiro[cyclohexane-1,3'-indolin]-4-one (8)*: White solid,  $^1\text{H}$  NMR ( $\text{CDCl}_3$ , 500 MHz),  $\delta$  2.13 (6 H, s), 2.77 (2H, dd,  $J=15.6, 4.1$  Hz), 2.98 (3 H, s), 3.42 (2 H, t,  $J=15.2$  Hz), 4.09 (2H, dd,  $J=14.5, 4.2$  Hz), 6.62 (1H, d,  $J=6.1$  Hz), 6.68 (4 H, d,  $J=8.0$  Hz), 6.74 (4 H, d,  $J=7.9$  Hz), 7.31–7.41



(2H, m), 8.01 (1H, d,  $J = 7.2$  Hz).  $^{13}\text{C}$  NMR ( $\text{CDCl}_3$ , 125.8 MHz):  $\delta$  20.8, 31.0, 44.9, 51.7, 67.8, 110.0, 123.2, 125.3, 128.1, 128.3, 128.7, 132.5, 134.6, 136.6, 146.2, 204.5, 208.1. HRMS (EI):  $m/z$  425.1796 ( $\text{M}^+ \text{C}_{28}\text{H}_{27}\text{NOS}^+$  requires 425.1813).

(1*s*,2*R*,6*S*)-1'-methyl-2,6-bis(4-nitrophenyl)-2'-thioxospiro[cyclohexane-1,3'-indolin]-4-one (9): Brown solid,  $^1\text{H}$  NMR ( $\text{CDCl}_3$ , 500 MHz)  $\delta$  2.81 (2H, dd,  $J = 15.6, 3.2$  Hz), 3.00 (3H, s), 3.47 (2H, t,  $J = 15.2$  Hz), 4.13 (2H, dd,  $J = 14.5, 3.5$  Hz), 6.76 (1H, d,  $J = 6.3$  Hz), 7.59–7.58 (2H, m), 7.68 (4H, d,  $J = 8.5$  Hz), 7.91 (4H, d,  $J = 8.5$  Hz) 8.16 (1H, dd,  $J = 4.9, 1.9$  Hz).  $^{13}\text{C}$  NMR ( $\text{CDCl}_3$ , 125.8 MHz):  $\delta$  34.6, 43.7, 49.8, 67.6, 108.5, 123.3, 125.5, 127.3, 128.5, 128.6, 129.5, 146.0, 146.9, 149.0, 207.7, 208.5. HRMS (EI):  $m/z$  487.1187 ( $\text{M}^+ \text{C}_{26}\text{H}_{21}\text{N}_3\text{O}_5\text{S}^+$  requires 487.1202).

(1*s*,2*R*,6*S*)-1'-2,6-triphenyl-2'-thioxospiro[cyclohexane-1,3'-indolin]-4-one (10): White solid,  $^1\text{H}$  NMR ( $\text{CDCl}_3$ , 500 MHz),  $\delta$  2.85 (2H, d,  $J = 14.5$  Hz), 3.50 (2H, t,  $J = 15.0$  Hz), 4.16 (2H, d,  $J = 14.1$  Hz), 6.20 (3H, s), 7.32 (8H, s), 7.53–7.56 (11H, m), 8.06 (1H, d,  $J = 7.3$  Hz).  $^{13}\text{C}$  NMR ( $\text{CDCl}_3$  and  $d_6$ -DMSO, 125.8 MHz):  $\delta$  43.3, 50.5, 66.6, 109.5, 112.5, 122.3, 125.8, 126.7, 127.3, 127.4, 127.4, 128.3, 130.6, 133.3, 135.1, 135.3, 145.6, 204.4, 208.4. HRMS (EI):  $m/z$  459.1553 ( $\text{M}^+ \text{C}_{31}\text{H}_{25}\text{NOS}^+$  requires 459.1657).

(1*s*,2*R*,6*S*)-2,6-bis(4-ethoxyphenyl)-1'-phenyl-2'-thioxospiro[cyclohexane-1,3'-indolin]-4-one (11): White solid,  $^1\text{H}$  NMR ( $\text{CDCl}_3$ , 500 MHz),  $\delta$  1.34 (6H, s), 2.83 (2H, d,  $J = 14.7$ ), 3.48 (2H, t,  $J = 15.0$ ), 3.91 (4H, s), 4.14 (2H, d,  $J = 13.3$ ), 6.19 (1H, d), 6.28 (2H, s), 6.54 (4H, d,  $J = 7.6$ ), 6.81 (4H, d,  $J = 7.4$ ), 7.21 (1H, t), 7.33 (4H, s), 8.04 (1H, d,  $J = 6.6$ ).  $^{13}\text{C}$  NMR ( $\text{CDCl}_3$ , 125.8 MHz):  $\delta$  13.5, 43.5, 50.0, 61.8, 67.0, 109.5, 112.0, 122.4, 124.6, 125.9, 127.5, 127.7, 128.3, 128.4, 128.5, 130.7, 135.1, 145.6, 156.7, 204.7, 208.6. HRMS (EI):  $m/z$  547.2187 ( $\text{M}^+ \text{C}_{35}\text{H}_{33}\text{NO}_3\text{S}^+$  requires 547.2176).

(1*s*,2*R*,6*S*)-1'-phenyl-2'-thioxo-2,6-di-*p*-tolylspiro[cyclohexane-1,3'-indolin]-4-one (12): White solid,  $^1\text{H}$  NMR ( $\text{CDCl}_3$ , 500 MHz),  $\delta$  2.23 (6H, s), 2.88 (2H, d,  $J = 14.5$  Hz), 3.53 (2H, t,  $J = 14.7$  Hz), 4.18 (2H, d,  $J = 14.2$  Hz), 6.23 (3H, s), 6.83 (8H, dd,  $J = 25.0$  Hz), 7.34 (5H, m), 8.08 (1H, d,  $J = 7.2$  Hz).  $^{13}\text{C}$  NMR ( $\text{CDCl}_3$  and  $d_6$ -DMSO, 125.8 MHz):  $\delta$  20.3, 44.0, 51.2, 67.3, 110.2, 113.2, 123.0, 126.5, 127.1, 128.0, 128.1, 128.3, 129.0, 134.0, 135.8, 136.0, 146.4, 205.2, 207.1. HRMS (EI):  $m/z$  487.1959 ( $\text{M}^+ \text{C}_{35}\text{H}_{33}\text{NO}_3\text{S}^+$  requires 487.1970).

(1*s*,2*R*,6*S*)-2,6-bis(4-nitrophenyl)-1'-phenyl-2'-thioxospiro[cyclohexane-1,3'-indolin]-4-one (13): Brown solid,  $^1\text{H}$  NMR ( $\text{CDCl}_3$ , 500 MHz)  $\delta$  2.95 (2H, dd,  $J = 15.5, 3.2$  Hz), 3.60 (2H, t,  $J = 15.3$  Hz), 4.26 (2H, dd,  $J = 14.5, 3.3$  Hz), 6.72 (3H, s), 7.78–7.89 (5H, m), 7.98 (4H, d,  $J = 8.5$  Hz), 8.01 (4H, d,  $J = 8.5$  Hz) 8.15 (1H, dd,  $J = 4.4, 1.7$  Hz).  $^{13}\text{C}$  NMR ( $\text{CDCl}_3$ , 125.8 MHz):  $\delta$  43.7, 49.8, 67.3, 112.7, 123.3, 125.4, 126.4, 127.4, 128.2, 128.6, 128.6, 129.1, 131.3, 139.4, 142.6, 146.0, 149.0, 207.0, 208.5. HRMS (EI):  $m/z$  549.1361 ( $\text{M}^+ \text{C}_{31}\text{H}_{23}\text{N}_3\text{O}_5\text{S}^+$  requires 549.1358).

Received: 12 September 2021; Accepted: 2 November 2021

Published online: 24 November 2021

## References

- Bassyouni, F. H., Hefnawi, M. E., Rashed, A. E. & Rehim, M. A. Molecular modeling and biological activities of new potent anti-microbial, anti-inflammatory and anti-nociceptive of 5-nitro indoline-2-one derivatives. *Drug Des.* **6**, 1000148. <https://doi.org/10.4172/2169-0138.1000148> (2017).
- Brahmachari, G. & Banerjee, B. Facile and one-pot access of 3,3-bis(indol-3-yl)indolin-2-ones and 2,2-bis(indol-3-yl)acenaphthylene-1(2h)-one derivatives via an eco-friendly pseudo-multicomponent reaction at room temperature using sulfamic acid as an organo-catalyst. *ACS Sustain. Chem. Eng.* **2**, 2802–2812. <https://doi.org/10.1021/sc500575h> (2014).
- Venkatesan, H., Davis, M. C., Altas, Y., Snyder, J. P. & Liotta, D. C. Total synthesis of SR 121463 A, a highly potent and selective vasopressin v2 receptor antagonist. *J. Org. Chem.* **66**, 3653–3661. <https://doi.org/10.1021/jo0004658> (2001).
- Sakai, S. *et al.* Gardneria alkaloids, part 9. Structures of chitosenine and three other minor bases: From gardneria multiflora makino. *Tetrahedron Lett.* **16**, 715–718. <https://doi.org/10.1002/chin.197526425> (1975).
- Sakai, S.-I., Aimi, N., Yamaguchi, K., Yamanaka, E. & Haginiwa, J. Gardneria alkaloids. Part 13. Structure of gardmultine and demethoxygardmultine; bis-type indole alkaloids of gardneria multiflora makino. *J. Chem. Soc., Perkin Trans. 1*, 1257–1262. <https://doi.org/10.1039/P19820001257> (1982).
- Rottmann, M. *et al.* Spiroindolones, a potent compound class for the treatment of malaria. *Science* **329**, 1175–1180. <https://doi.org/10.1126/science.1193225> (2010).
- Dideberg, O. *et al.* Structure cristalline et moléculaire d'un nouvel alcaloïde bisindolique: complexe moléculaire 1:2 strychnofoline-éthanol ( $\text{C}_{30}\text{H}_{34}\text{N}_4\text{O}_2 \cdot 2\text{C}_2\text{H}_6\text{O}$ ). *Acta Cryst.* **B33**, 1796–1801. <https://doi.org/10.1107/S0567740877007080> (1977).
- Subramaniam, G. *et al.* Biologically active aspidofractinine, rhazinilam, akuammiline, and vincorine alkaloids from kopsia. *J. Nat. Prod.* **70**, 1783–1789. <https://doi.org/10.1021/np0703747> (2007).
- Janin, Y. L. Antituberculosis drugs: Ten years of research. *Biorg. Med. Chem.* **15**, 2479–2513. <https://doi.org/10.1016/j.bmc.2007.01.030> (2007).
- Gutierrez-Lugo, M.-T. & Bewley, C. A. Natural products, small molecules, and genetics in tuberculosis drug development. *J. Med. Chem.* **51**, 2606–2612. <https://doi.org/10.1021/jm070719i> (2008).
- Zea, A., Alba, A.-N.R., Mazzanti, A., Moyano, A. & Rios, R. Highly enantioselective cascade synthesis of spiropyrazolones. *Org. Biomol. Chem.* **9**, 6519–6523. <https://doi.org/10.1039/C1OB05753G> (2011).
- Zhu, C.-L. *et al.* Enantioselective base-free electrophilic amination of benzofuran-2(3h)-ones: Catalysis by binol-derived p-spiro quaternary phosphonium salts. *Angew. Chem. Int. Ed.* **50**, 5869–5872. <https://doi.org/10.1002/anie.201100283> (2011).
- Bondock, S., Rabie, R., Etman, H. A. & Fadda, A. A. Synthesis and antimicrobial activity of some new heterocycles incorporating antipyrine moiety. *Eur. J. Med. Chem.* **43**, 2122–2129. <https://doi.org/10.1016/j.ejmech.2007.12.009> (2008).
- Wan, J.-P., Lin, Y., Huang, Q. & Liu, Y. Diastereoselective construction of tetrahydropyridine fused bicyclic structures via three-component domino reaction. *J. Org. Chem.* **79**, 7232–7238. <https://doi.org/10.1021/jo501292q> (2014).
- Chen, X.-B., Liu, Z.-C., Yang, L.-F., Yan, S.-J. & Lin, J. A Three-component catalyst-free approach to regioselective synthesis of dual highly functionalized fused pyrrole derivatives in water-ethanol media: Thermodynamics versus kinetics. *ACS Sustain. Chem. Eng.* **2**, 1155–1163. <https://doi.org/10.1021/sc500170d> (2014).
- Song, Z., Huang, X., Yi, W. & Zhang, W. One-pot reactions for modular synthesis of polysubstituted and fused pyridines. *Org. Lett.* **18**, 5640–5643. <https://doi.org/10.1021/acs.orglett.6b02883> (2016).
- Mancebo-Aracil, J., Nájera, C. & Sansano, J. M. Multicomponent synthesis of unnatural pyrrolizidines using 1,3-dipolar cycloaddition of proline esters. *Chem. Commun.* **49**, 11218–11220. <https://doi.org/10.1039/C3CC47184E> (2013).

18. Zhang, X., Legris, M., Muthengi, A. & Zhang, W. [3+2] Cycloaddition-based one-pot synthesis of 3,9-diazabicyclo[4.2.1]nonane-containing scaffold. *Chem. Heterocycl. Compd.* **53**, 468–473. <https://doi.org/10.1007/s10593-017-2072-2> (2017).
19. Selva, V. *et al.* Diastereoselective [3 + 2] vs [4 + 2] cycloadditions of nitroprolates with  $\alpha$ ,  $\beta$ -unsaturated aldehydes and electrophilic alkenes: An example of total periselectivity. *J. Org. Chem.* **82**, 6298–6312. <https://doi.org/10.1021/acs.joc.7b00903> (2017).
20. Zhang, X. *et al.* One-pot double [3 + 2] cycloadditions for diastereoselective synthesis of pyrrolidine-based polycyclic systems. *J. Org. Chem.* **83**, 13536–13542. <https://doi.org/10.1021/acs.joc.8b02046> (2018).
21. Yamazaki, T., Shinohara, N., Kitazume, T. & Sato, S. Highly diastereoselective sequential enolate-Michael addition-ireland Claisen rearrangement. *J. Org. Chem.* **60**, 8140–8141. <https://doi.org/10.1021/jo00130a012> (1995).
22. Srivastava, N. & Banik, B. K. Bismuth nitrate-catalyzed versatile Michael reactions. *J. Org. Chem.* **68**, 2109–2114. <https://doi.org/10.1021/jo026550s> (2003).
23. Krause, N. & Hoffmann-Röder, A. Recent advances in catalytic enantioselective Michael additions. *Synthesis* **0171–0196**, 2001. <https://doi.org/10.1055/s-2001-10803> (2001).
24. Okino, T., Hoashi, Y. & Takemoto, Y. Enantioselective Michael reaction of malonates to nitroolefins catalyzed by bifunctional organocatalysts. *J. Am. Chem. Soc.* **125**, 12672–12673. <https://doi.org/10.1021/ja036972z> (2003).
25. Sivasankara, C., Satham, L. & Namboothiri, I. N. N. One-pot construction of functionalized spiro-dihydronaphthoquinone-oxindoles via Hauser–Kraus annulation of sulfonylphthalide with 3-alkylideneoxindoles. *J. Org. Chem.* **82**, 12939–12944. <https://doi.org/10.1021/acs.joc.7b02656> (2017).
26. Wang, L.-L. *et al.* Highly organocatalytic asymmetric Michael–ketone aldol–dehydration domino reaction: Straightforward approach to construct six-membered spirocyclic oxindoles. *Chem. Commun.* **46**, 8064–8066. <https://doi.org/10.1039/C0CC03032E> (2010).
27. Ball-Jones, N. R., Badillo, J. J. & Franz, A. K. Strategies for the enantioselective synthesis of spirooxindoles. *Org. Biomol. Chem.* **10**, 5165–5181. <https://doi.org/10.1039/C2OB25184A> (2012).
28. Cheng, D., Ishihara, Y., Tan, B. & Barbas, C. F. Organocatalytic asymmetric assembly reactions: Synthesis of spirooxindoles via organocascade strategies. *ACS Catal.* **4**, 743–762. <https://doi.org/10.1021/cs401172r> (2014).
29. Li, Z., Li, J. & Yang, J. Chemoselective double Michael addition: Synthesis of 2,6-diarylspiro[cyclohexane-1,3'-indoline]-2',4'-diones via addition of indolin-2-one to divinyl ketones. *J. Chem. Res.* **41**, 168–171. <https://doi.org/10.3184/174751917X14878812592779> (2017).
30. Wu, B. *et al.* Highly enantioselective synthesis of spiro[cyclohexanone-oxindoles] and spiro[cyclohexanone-pyrazolones] by asymmetric cascade [5+1] double Michael reactions. *Eur. J. Org. Chem.* **1318–1327**, 2012. <https://doi.org/10.1002/ejoc.201101529> (2012).
31. Géant, P.-Y., Urban, M., Remeš, M., Čisářová, I. & Veselý, J. Enantioselective organocatalytic synthesis of sulfur-containing spirocyclic compounds. *Eur. J. Org. Chem.* **7979–7988**, 2013. <https://doi.org/10.1002/ejoc.201300931> (2013).
32. Scala, A. *et al.* Direct synthesis of C3-mono-functionalized oxindoles from N-unprotected 2-oxindole and their antileishmanial activity. *Biorg. Med. Chem.* **22**, 1063–1069. <https://doi.org/10.1016/j.bmc.2013.12.039> (2014).
33. Saha, S. *et al.* A novel spirooxindole derivative inhibits the growth of *Leishmania donovani* parasites both in vitro and in vivo by targeting type I topoisomerase. *Antimicrob. Agents Chemother.* **60**, 6281–6293. <https://doi.org/10.1128/AAC.00352-16> (2016).
34. Pulvertaft, R. J. V. & Hoyle, G. F. Stages in the life-cycle of *Leishmania donovani*. *Trans. R. Soc. Trop. Med. Hyg.* **54**, 191–196. [https://doi.org/10.1016/0035-9203\(60\)90057-2](https://doi.org/10.1016/0035-9203(60)90057-2) (1960).
35. French, J. B. *et al.* The *Leishmania donovani* UMP synthase is essential for promastigote viability and has an unusual tetrameric structure that exhibits substrate-controlled oligomerization. *J. Biol. Chem.* **286**, 20930–20941. <https://doi.org/10.1074/jbc.M111.228213> (2011).
36. Moghaddam, F. M., Khodabakhshi, M. R., Kiamehr, M. & Ghahremannejad, Z. Synthesis of novel pentacyclic thiopyrano indole-annulated benzo- $\delta$ -sultone derivatives via a domino Knoevenagel-hetero-Diels–Alder reaction in water. *Tetrahedron Lett.* **54**, 2685–2689. <https://doi.org/10.1016/j.tetlet.2013.03.070> (2013).
37. Moghaddam, F. M., Saeidian, H., Mirjafary, Z., Taheri, S. & Kheirjou, S. A new and facile synthesis of thieno[2,3-b]indole derivatives via condensation of isocyanide and indolin-2-thiones. *Synlett* **1047–1050**, 2009. <https://doi.org/10.1055/s-0028-1088107> (2009).
38. Pettersen, E. F. *et al.* UCSF Chimera—A visualization system for exploratory research and analysis. *J. Comput. Chem.* **25**, 1605–1612. <https://doi.org/10.1002/jcc.20084> (2004).
39. Goodsell, D. S. & Olson, A. J. Automated docking of substrates to proteins by simulated annealing. *Proteins: Struct. Funct. Genet.* **8**, 195–202. <https://doi.org/10.1002/prot.340080302> (1990).
40. Keith, T. A. & Millam, J. M. *GaussView, Version 6.1*, Roy Dennington (Semichem Inc, 2016).
41. Cossi, M. & Barone, V. Time-dependent density functional theory for molecules in liquid solutions. *J. Chem. Phys.* **115**, 4708–4717. <https://doi.org/10.1063/1.1394921> (2001).
42. Zhao, Y., Schultz, N. E. & Truhlar, D. G. Exchange-correlation functional with broad accuracy for metallic and nonmetallic compounds, kinetics, and noncovalent interactions. *J. Chem. Phys.* **123**, 161103. <https://doi.org/10.1063/1.2126975> (2005).
43. Hariharan, P. C. & Pople, J. A. The influence of polarization functions on molecular orbital hydrogenation energies. *Theor. Chim. Acta* **28**, 213–222. <https://doi.org/10.1007/BF00533485> (1973).
44. Hefre, W., Yu, J., Klunzinger, P. & Lou, L. *Spartan Software. Wavefunction* (Irvine Inc, 2000).
45. Frisch, M. J. *et al.* *Gaussian 16, Revision A.03* (Gaussian Inc, 2010).
46. Sheldrick, G. M. SHELXT—Integrated space-group and crystalstructure determination. *Acta Cryst.* **A71**, 3–8. <https://doi.org/10.1107/S2053273314026370> (2015).
47. Sheldrick, G. M. Crystal structure refinement with SHELXL. *Acta Cryst.* **C71**, 3–8. <https://doi.org/10.1107/S2053229614024218> (2015).
48. Spek, A. L. Structure validation in chemical crystallography. *Acta Cryst.* **D65**, 148–155. <https://doi.org/10.1107/S090744490804362X> (2009).
49. Macrae, C. F. *et al.* Mercury CSD 2.0—New features for the visualization and investigation of crystal structures. *Appl. Cryst.* **41**, 466–470. <https://doi.org/10.1107/S0021889807067908> (2008).
50. Kondhare, D., Deshmukh, S. & Lade, H. Curcumin analogues with aldose reductase inhibitory activity: Synthesis, biological evaluation, and molecular docking. *Processes* **7**, 417. <https://doi.org/10.3390/pr7070417> (2019).
51. Mane, V., Baiju, T. V. & Namboothiri, N. N. Synthesis of functionalized thieno[2,3-b]indoles via one-pot reaction of indoline-2-thiones with Morita–Baylis–Hillman and Rauhut–Currier adducts of nitroalkenes. *ACS Omega* **3**, 17617–17628. <https://doi.org/10.1021/acs.omega.8b02147> (2018).
52. Moghaddam, F. M. *et al.* Facile entry to polycyclic indolylhydroquinoline skeletons via tandem C-alkylation and intramolecular S-alkylation. *Tetrahedron* **66**, 134–138. <https://doi.org/10.1016/j.tet.2009.11.032> (2010).

## Acknowledgements

We thank Prof. Yvan Six for 2D NMR experiments and HRMS analysis and Marie Cordier for X-ray crystallography analysis. Financial support was provided by Sharif University of Technology, McGill University, and the Iran National Science Foundation Grant to F.M.M for funding.

### Author contributions

F.M.M. and V.S. conceived the project. V.S. and A.K. collected and analyzed the data. All authors contributed to experimental design and manuscript writing.

### Competing interests

The authors declare no competing interests.

### Additional information

**Supplementary Information** The online version contains supplementary material available at <https://doi.org/10.1038/s41598-021-01766-6>.

**Correspondence** and requests for materials should be addressed to F.M.M.

**Reprints and permissions information** is available at [www.nature.com/reprints](http://www.nature.com/reprints).

**Publisher's note** Springer Nature remains neutral with regard to jurisdictional claims in published maps and institutional affiliations.



**Open Access** This article is licensed under a Creative Commons Attribution 4.0 International License, which permits use, sharing, adaptation, distribution and reproduction in any medium or format, as long as you give appropriate credit to the original author(s) and the source, provide a link to the Creative Commons licence, and indicate if changes were made. The images or other third party material in this article are included in the article's Creative Commons licence, unless indicated otherwise in a credit line to the material. If material is not included in the article's Creative Commons licence and your intended use is not permitted by statutory regulation or exceeds the permitted use, you will need to obtain permission directly from the copyright holder. To view a copy of this licence, visit <http://creativecommons.org/licenses/by/4.0/>.

© The Author(s) 2021